SIAM J. Applied Dynamical Systems
Vol. 12, No. 1, pp. 515–532

Multiparameter Models of Innovation Diffusion on Complex Networks*

N. J. McCullen†, A. M. Rucklidge‡, C. S. E. Bale§, T. J. Foxon¶, and W. F. Gale§

Abstract. A model, applicable to a range of innovation diffusion applications with a strong peer-to-peer component, is developed and studied, along with methods for its investigation and analysis. A particular application is to individual households deciding whether to install an energy efficiency measure in their home. The model represents these individuals as nodes on a network, each with a variable representing their current state of adoption of the innovation. The motivation to adopt is composed of three terms, representing personal preference, an average of each individual's network neighbors' states, and a system average, which is a measure of the current social trend. The adoption state of a node changes if a weighted linear combination of these factors exceeds some threshold. Numerical simulations have been carried out, computing the average uptake after a sufficient number of time-steps over many randomizations at all model parameter values, on various network topologies, including random (Erdős–Rényi), small world (Watts–Strogatz), and (Newman) highly clustered, community-based networks. An analytical and probabilistic approach has been developed to account for the observed behavior, which explains the results of the numerical calculations.

Key words. innovation diffusion, networks, threshold models, uptake of energy efficiency measures

AMS subject classifications. 91-04, 91F99

DOI. 10.1137/120885371

1. Introduction.

Social phenomena, such as the spread of a technological or behavioral innovation through communities, can be modeled as dynamical processes on networks [1, 6, 7, 8, 9, 17]. Our model, introduced in section 2, builds on previous threshold diffusion models (see, e.g., [8, 20, 27]) by incorporating sociologically realistic factors yet remains simple enough for mathematical insights to be developed.

An example of a particular application of this model is the adoption of innovations related to energy behaviors and technologies by individual households. These innovations are often not directly visible to an adopter's peers, but communication of the benefits of adoption may occur through interaction between individuals. The decision to adopt is therefore based on multiple factors, taking into account not only individual preferences but also whether or not an individual's social circle has adopted the innovation. As such, the spread of the innovation will be influenced by the network of social contacts between individuals, including both social peers and wider social trends. Models have been developed along these lines [5], splitting the

*Received by the editors July 20, 2012; accepted for publication (in revised form) by M. Golubitsky January 14, 2013; published electronically March 26, 2013. This work was funded under the EPSRC Energy Challenges for Complexity Science panel, grant EP/G059780/1.
http://www.siam.org/journals/siads/12-1/88537.html
†Research Unit for Energy and the Design of Environments, University of Bath, Bath, UK (n.mccullen@physics.org).
‡Department of Applied Mathematics, University of Leeds, Leeds, UK (a.m.rucklidge@leeds.ac.uk).
§Energy Research Institute, University of Leeds, Leeds, UK (c.s.e.bale@leeds.ac.uk, w.f.gale@leeds.ac.uk).
¶School of Earth and Environment, University of Leeds, Leeds, UK (t.j.foxon@leeds.ac.uk).

influence on individual decision-making between various social factors, and show interesting dynamics in looking at the balance of these influences. The real topologies of interpersonal networks are not known exactly and are constantly changing, further adding to the uncertainty in models of social phenomena. Given these challenges, useful models and methods are required that can assess the likely outcomes of particular scenarios, such as the effect of an intervention to persuade a population to adopt an innovation, without being excessively sensitive to particular choices of parameter values of the model or the precise structure of the network. Here, we present numerical investigations of the model, studying its behavior statistically as well as presenting mathematical analysis that gives a deeper understanding of the observed uptake of the innovation over the network using probabilistic arguments.

The numerical methods used in section 3 take the ensemble averages of simulation outcomes over many realizations, each with different conditions, such as the initial seed of adopters or the precise details of the network structure. This is carried out over a range of parameter values and on different types of network topologies in order to study both the stability of the model with respect to minor variations and the sensitivity to structural details of the models used. These methods can therefore be applied to various dynamical models on a variety of networks to assess likely differences in outcomes for alternative scenarios in a statistical sense, rather than relying on individual predictions.

We take the applied dynamical systems approach of looking for lines in parameter space where the behavior of the dynamical process changes. Mathematical analysis is presented in section 4 explaining observations for the simulation results in certain simplified cases. Specifically, assuming that all individuals are homogeneous in their model parameters, we can use probabilistic arguments for the conditions of the neighborhoods of the individuals required to trigger uptake, and we calculate the likelihood of success given a choice of parameters on certain types of networks.

We have found that the likelihood of success, defined as adoption by the majority of individuals, depends strongly on both the choice of model parameters and the topology of the network. Two particularly important factors are found to be the *node degree*, i.e., the number of connections of the nodes with their neighbors, and the network's *transitivity*, which is the degree of clustering related to the correlation between the neighborhoods of connected individuals. This makes it possible to assess what changes to the model would result in an increased probability of success and how this can be interpreted in terms of policy decisions intent on maximizing adoption in the real world.

2. Modeling social behavior as dynamical systems on networks. A system of N individuals (or groups such as households) can be represented by N *nodes* on a *network*. Possible interactions linking individuals are represented by the *edges* on the network. The network topology can be represented in the *adjacency matrix* A, an N^2 matrix with entries:

$$A_{ij} = \begin{cases} 1 & \text{if node } j \text{ influences } i, \\ 0 & \text{otherwise.} \end{cases} \tag{2.1}$$

Information or influence is passed along these edges, which could also be given weights to show the relative probability or strength of the interaction. In this work all influences are taken to be of equal weight and symmetric in both directions. States are assigned to the nodes,

describing the properties of the individuals, and deterministic or probabilistic equations or rules can be used to describe the evolution of these states over time.

2.1. A multiparameter model for innovation uptake. The following model describes the purchase or adoption of a single innovation (not considering competition between similar items) but could apply equally well to the spread of any property over a network, such as a rumor or behavior. The model used in this work assigns each node i a binary variable representing their current state, $x_i = 1, 0$, indicating whether or not the individual has adopted the innovation. The nodes in state $x = 1$ are referred to as *activated* nodes. The initial state is a fixed proportion of activated nodes, randomly distributed across the network. The decision to invest in the innovation is determined by the perceived usefulness, or *utility*, to the individual (which can include subjective judgements). When this utility outweighs the barriers to adoption (including financial costs), the individual i adopts the innovation, so x_i changes from 0 to 1. As this is a one-way process, unlike voter models [7], the state at the next time-step is determined by

$$x_i(t+1) = \begin{cases} 1 & \text{if } x_i(t) = 1, \\ 1 & \text{if } x_i(t) = 0 \text{ and } u_i(t) > \theta_i, \\ 0 & \text{otherwise,} \end{cases} \tag{2.2}$$

where θ_i is the threshold and t is time. All nodes are updated synchronously at each time-step in the current work. The total utility u_i is a combination of both personal and social benefits [9]. The personal benefit p_i is a measure of the perceived intrinsic benefit to the individual of acquiring the innovation. The social benefit can be split into both the direct influence from an individual's peer group and the (possibly indirect) influence from society in general [25], which could be affected by the desire to fit in with the social norm on different levels. Thus our utility model has three factors that can be given relative weightings α_i, β_i, and γ_i, with $\alpha_i + \beta_i + \gamma_i = 1$. The total utility is, therefore, given by

$$u_i(t) = \alpha_i p_i + \beta_i s_i(t) + \gamma_i m(t), \tag{2.3}$$

where s_i is the average of x within a node's *network neighborhood*,

$$s_i(t) = \frac{1}{k_i} \sum_{j}^{N} A_{ij} x_j(t), \tag{2.4}$$

and the *degree* of node i is $k_i = \sum_{j=1}^{N} A_{ij}$. The mainstream social norm m is the average of x over the entire population:

$$m(t) = \frac{1}{N} \sum_{i}^{N} x_i(t). \tag{2.5}$$

This can be made equivalent to previous threshold diffusion models such as [27] by setting $(\alpha, \beta, \gamma) = (0, 1, 0)$. We define $m_0 = m(t = 0)$ to be the initial fraction of adopters. For the rest of the discussion we make the simplifying assumption that all nodes take the same values of α, β, γ, p, and θ, so that only the value of $s_i(t)$ differs between the nodes, which corresponds to the network effects.

2.2. Modeling social networks. For these investigations we connected the nodes using several network models. Random *Erdős–Rényi* (ER) graphs [12], where edges are connected with a probability p_e between pairs of nodes, were investigated for their analytical simplicity, due to the lack of correlation between neighborhoods of nodes, allowing probabilistic arguments to be used [16]. The *Watts–Strogatz* scheme [28], where n-nearest-neighbor lattices have edges removed and reassigned according to a probability p_r, allowing interpolation between regular (possibly highly clustered) topologies and random networks, was also investigated, as it is frequently studied and provides a simple way to vary the clustering (*transitivity*) of the system.

Empirical studies have shown that real-world networks are often organized into *communities* of subnetworks [23], which are more densely connected internally than to the rest of the network, and models exist showing mechanisms that can result in the formation of such communities [21]. *Community-based models*, such as Newman's highly clustered networks [22], can better represent real-world social interactions in a number of ways. Here, links between nodes are assigned via their association with G *groups* each, which are randomly chosen from a set of W groups in total. Association with two or more groups per node is necessary for the network to be fully connected and total transmission to be possible. Nodes are linked to L other nodes within each group, so the total number of groups W and resulting number of members of each group $M = GN/W$ provide a means of varying the clustering while keeping other network parameters fixed. These networks also have locally higher clustering between members of a group than out to the rest of the network. For these models it would also be possible to give some geographical information to the nodes and groups in the network (cf. Hamill and Gilbert's *social circles* model [19]), as discussed further in section 5.

Networks with *scale-free* degree distributions are also widely used in the literature, such as the *Barabási–Albert* (preferential attachment) model. Such degree distributions exist when considering the complete peer-networks of individuals, including both strong and weak links. However, in the application motivating this research, where individuals recommend a certain innovation to their peers, it is reasonable to assume that people discuss financial matters and share recommendations with only a core group of associates, allowing us to ignore the more numerous weaker links. It has previously been shown that adoption decisions are influenced via the strongest links in the network rather than all *weak ties* [29]. This is backed up by a survey we conducted on residents of the city of Leeds, where individuals reported limited communications with their peers on issues of energy and saving money [4]. We show how including such links would affect our results due to the skewed nature of the fat-tail of the degree distributions.

3. Numerical methods. In order to investigate the diffusion dynamics of the system, we performed simulations on various networks, using a synchronous updating rule for the states of the nodes. Given a particular network, initial set of adopters, and parameter values $(\alpha, \beta, \gamma, p, \theta)$, we ask whether or not the innovation *succeeds*. That is, do most individuals adopt the innovation? Aside from the challenges inherent in modeling the complex factors affecting behavior, as well as in quantifying models from social data, dynamical processes on complex networks themselves often exhibit dependence on the starting conditions, such as which nodes are chosen as the initial seed. To illustrate the sensitivity to the precise starting

conditions, the simulation results for a particular network and a single choice of parameters are given in Figure 1(a), showing the uptake over 36 time steps for 100 random realizations of the initial seed. In each case, 5% of the nodes are chosen as *seed nodes* at random and are set to 1, with the rest initialized at 0. It can clearly be seen that while many runs quickly lead to successful adoption, defined as most or all nodes becoming active, there is a clear subset of about 44% of initial conditions that stagnates and does not take over an appreciable proportion of the network. In cases of stagnation the dynamics of the current model become frozen in a small number of time-steps, and no more adoption takes place, due to the static nature of the network and deterministic rules used.

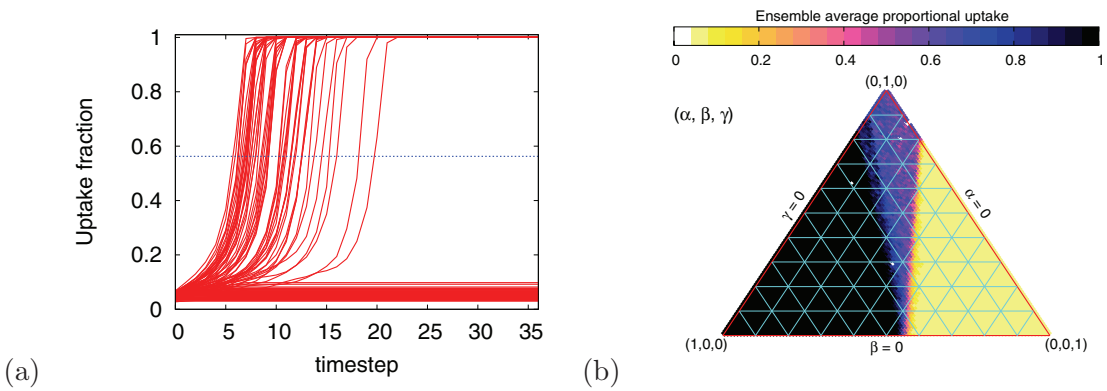

Figure 1. *Simulations of the adoption model on a community based network, with* $N = 500$ *nodes linked to others via their shared association with groups. Each node is randomly assigned to* $G = 2$ *groups, from a total of* $W = 100$*, and is linked with* $L = 5$ *other nodes per group.* (a) *Runs starting from* 100 *realizations of a* 5% *level of initial adoption* ($m_0 = 0.05$)*, with model parameters* $\alpha = 0.1, \beta = 0.8, \gamma = 0.1, p = 0.5, \theta = 0.25$*. The mean uptake over the* 100 *realizations at time-step* 36 *is* 56%. (b) *The mean uptake at values in the* β, γ *parameter space, with* $\alpha = 1 - \beta - \gamma$*. All nodes take the same parameter values as each other.*

Given that this sensitivity can result in a wide range of uptake levels, we focus on estimating the likelihood of success for a model run, rather than the expected level of success for a particular run. To obtain this, the ensemble average uptake over 100 realizations of the choice of seed nodes is computed for each chosen set of parameter values. The detailed structure of the network is randomized at each set of parameter values. In order to look at the influence of the parameters on the expected uptake, this calculation is repeated over a range of parameter values and is plotted in the β, γ parameter space, with $0 \leqslant \beta \leqslant 1$, $0 \leqslant \gamma \leqslant 1$, and $\alpha = 1 - \beta - \gamma$. An example plot is shown in Figure 1(b). Two lines can be seen dividing regions of the parameter space where adoption is total (black), where uptake is about 65% (blue), and where it stagnates at levels up to only slightly above the initial seeding level of 5% (yellow).

4. Results and analysis. The procedure described in the previous section was carried out for different network topologies in order to investigate the general behavior of the model. The results all show distinct regions of either near-total success or stagnation, with a few exceptions where there is a region of intermediate probability of success. In this section we present the results of these simulations along with an analysis into the origin of the dividing lines between these regions in parameter space. This is presented first in terms of random ER

networks and later for other network models.

4.1. Number of neighbors needed to induce uptake. In order to understand which parameter values are likely to lead to a higher level of adoption, it is important to consider the properties of the nodes' local network environment. Each node experiences the same p and m in (2.3), so the only difference between the nodes is s_i, the fraction of its neighbors which are active. For any set of parameter values and current adoption level $m(t)$, there is a critical fraction $s^*(t)$, defined by

$$s^*(t) = \frac{\theta - \alpha p - \gamma m(t)}{\beta}, \tag{4.1}$$

such that if $s_i \geqslant s^*$, the node will adopt the innovation in the next time-step. The required number of active contacts Y_i^* (an integer) is given by

$$Y_i^*(t) = \lceil k_i s_i^*(t) \rceil, \tag{4.2}$$

where $\lceil \bullet \rceil$ denotes the smallest integer $\geqslant \bullet$. If the actual number of active contacts

$$Y_i = \sum_j A_{ij} x_j \tag{4.3}$$

is at least Y_i^*, then node i will take up the innovation in the next time-step. To simplify matters, we consider first networks where the nodes all have the same (or similar) degree $\bar{k}$, defined by

$$\bar{k} = \frac{1}{N} \sum_{ij} A_{ij}. \tag{4.4}$$

In this case we can define the critical number of active contacts to be

$$Y^* = \lceil \bar{k} s^*(t) \rceil = \left\lceil \bar{k} \left(\frac{\theta - \alpha p - \gamma m(t)}{\beta} \right) \right\rceil, \tag{4.5}$$

and the success or otherwise of the innovation uptake across the network can be understood in terms of Y^*. If $Y^* = 0$, then all nodes immediately adopt the innovation. If $Y^* = 1$, then any node connected to one of the initial seed nodes adopts the innovation, and the innovation uptake will be successful in a fully connected network. If $Y^* = 2$, then a node must be connected to two active nodes in order to adopt. We show below that for reasonable values of m_0, and for a wide class of networks, this leads to success. The case $Y^* = 3$ will also be discussed below.

Using $\alpha = 1 - \beta - \gamma$, (4.5) can be inverted to give

$$\beta = \bar{k} \left(\frac{\gamma(m(t) - p) + p - \theta}{\bar{k}p - Y^*} \right). \tag{4.6}$$

This gives, for different $m(t)$, and for different integers Y^*, a sequence of lines in the (β, γ) parameter plane. These lines (with $m(t) = m_0$) are overlaid on numerical results in Figure 2 for random ER networks of different sizes ($N = 500$, $N = 2000$) and different average degrees ($\bar{k} = 6$, $\bar{k} = 15$). In Figure 2(a) ($N = 500$, $\bar{k} = 6$), uptake is successful for most values of (β, γ) to the left of the $Y^* = 2$ line. This boundary becomes sharper for $N = 2000$ and agrees more closely with the theoretical $Y^* = 2$ line in Figure 2(b). For $\bar{k} = 15$, $N = 500$ (Figure 2(c)), it is the $Y^* = 3$ line that separates success from failure.

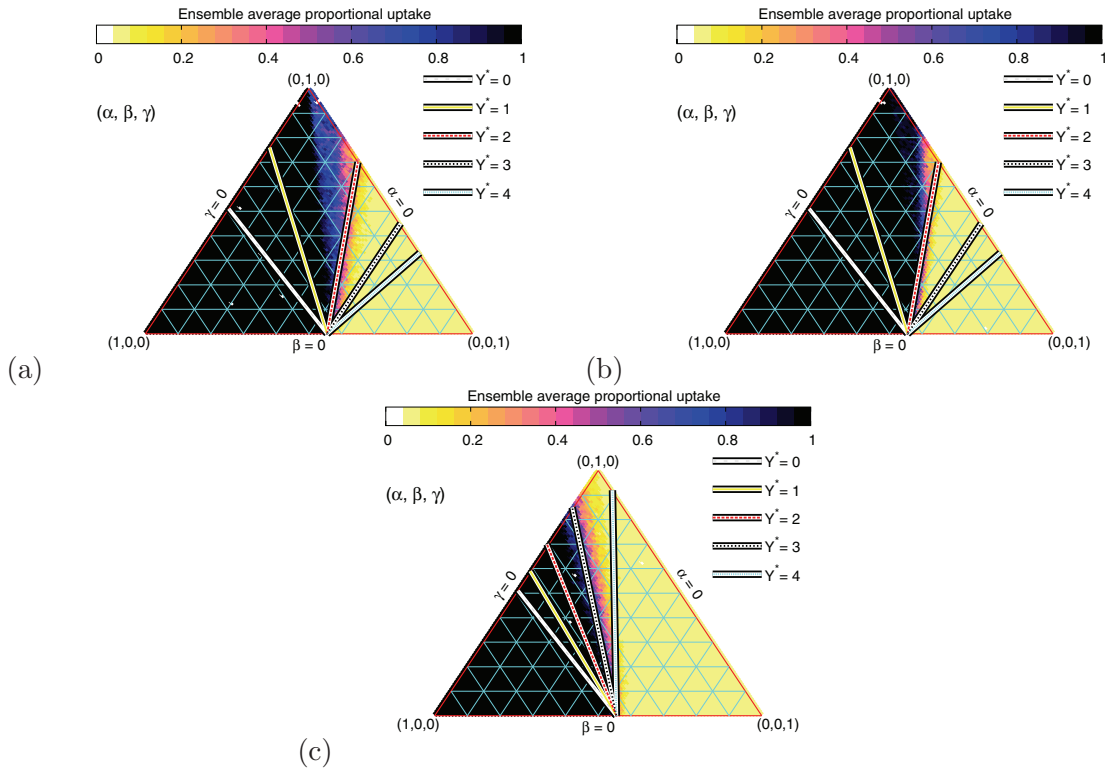

Figure 2. *Comparison of simulations of the adoption model on random ER networks. As in all cases* $\theta = 0.25$ *and* $p = 0.5$. *The mean node degree* $\bar{k}$ *and network size* N *values are* (a) $\bar{k} = 6$, $N = 500$; (b) $\bar{k} = 6$, $N = 2000$; (c) $\bar{k} = 15$, $N = 500$. *The results of the analysis in section* 4 *are also plotted for* $Y^* = 0, 1, 2, 3, 4$. *The lines of* Y^* *in the* (β, γ) *plane show the upper limits of* (β, γ) *for each value of the critical number of neighbors* Y^*. *For example, two active neighbors are required to trigger adoption to the left of the* $Y^* = 2$ *line, but this changes to three on the right side of the line.*

4.2. Probability of induced uptake in random networks. We begin by calculating the probability that the condition $Y_i \geqslant Y^*$ is satisfied. In the current context, where we consider the *initial* stages of propagation, the initial adopters are few in number and unlikely to be connected in the first instance. On finite size networks this is an important consideration, as it would determine whether the process stagnates in the early stages or has a chance of continuing through other mechanisms, such as via the *clustering* mechanism outlined in later sections. The assumption of nonoverlapping active neighborhoods is too strong to generalize to later stages in the process, particularly on highly clustered networks. However, on large random (i.e., *unclustered*) networks, it will remain valid for several time-steps, as the neighborhoods are uncorrelated and probabilities of active neighbors independent of one another. So for random networks with independent random assignment of initial conditions, where all nodes have a statistically homogeneous local network environment and the same node degree k, the probability of Y neighbors being active is given by a binomial distribution:

$$P(Y \geq Y^*) = \sum_{n=Y^*}^{k} \binom{k}{n} m^n (1-m)^{(k-n)}. \tag{4.7}$$

This is just the probability of at least Y^* nodes being adopters, from k nodes in the neighborhood, given that each node has a probability m of being an adopter. Clearly $P(Y \geq Y^*)$ is zero if $Y^* > k$.

For the specific examples in Figure 2 the outcomes in the different sectors of the parameter space can be understood using these ideas. If we define Z to be the number of nodes in the whole network whose neighborhood influences them to adopt, then the probability that at least one further node will be influenced somewhere in the network is $P(Z \geq 1) = 1 - P(Z = 0)$, where the probability that no neighborhoods are influential is $P(Z = 0) = (P(Y < Y^*))^N$, and $P(Y < Y^*) = 1 - P(Y \geqslant Y^*)$, which, using (4.7) gives the expression

$$P(Z \geq 1) = 1 - \left(1 - \sum_{n=Y^*}^{k} \binom{k}{n} m^n (1-m)^{(k-n)}\right)^N. \tag{4.8}$$

This can be seen to be a specific case of Gleeson's [13] and Gleeson and Cahalane's [15] equation (1), where average uptake levels are solved for the Watts 2002 model [27] (i.e., taking $\beta = 1$) on random networks with arbitrary degree distributions. Here we have restricted the analysis to a single node degree, rather than a distribution, for simplicity and to maintain consistency with the results in section 4.1.[1] Equation (4.8) works for the examples used here, which are limited to cases where there is a tightly bound node degree, but the more general formulation of Gleeson would most likely give more accurate results for the rates found within the different regions given by the analysis in section 4.1.

For small m (4.8) approximates to

$$P(Z \geq 1) \approx 1 - \left(1 - \binom{k}{Y^*} m^{Y^*}\right)^N. \tag{4.9}$$

For $k = 6$, $N = 500$, and $m_0 = 0.05$ this gives $P(Z \geq 1) \approx 1$ for both $Y^* = 1, 2$, but for $Y^* = 3$, $P(Z \geq 1) \approx 0.7$. For the $Y^* = 2$ case, the probability of a site having an influential neighborhood is $P(Y \geq Y^*) \approx 0.0375$, and the expected number of nodes satisfying this condition is this probability multiplied by the number of remaining (inactive) nodes $N(1-m)P(Y \geq Y^*) \approx 18$, doubling adoption at each time-step. However, in the $Y^* = 3$ sector, the probability of any chosen node having the required number of neighbors is $P(Y \geq Y^*) \approx 0.0025$, resulting in only one expected new active node with a network size $N = 500$, easily leading to stagnation. The $Y^* = 2$ line becomes a sharper dividing line for larger networks (Figure 2(b)), as finite size fluctuation effects become less important. The value of Y^* which is the dividing line changes for $\bar{k} = 15$ (Figure 2(c)), where $N(1-m)P(Y \geq Y^* = 3) \approx 27$, again of the order of the initial seeding level, and so adoption is successful for $Y^* = 3$ but fails when $Y^* = 4$.

4.3. Propagation on random networks. In (4.5), Y^* is a decreasing function of time, since $m(t)$ can only increase. As argued above, if $Y^* = 0$ or 1, uptake will be successful. In

[1] It would be possible to reformulate the results in section 4.1 in a similar spirit to Gleeson, but this would involve performing a weighted sum over a range of terms of the form of (4.5) for every degree in the distribution k_i rather than taking the mean value $\bar{k}$, greatly reducing the simplicity of the result demonstrated here.

this section, we estimate the likelihood that Y^* will decrease from a larger initial value to 1 and how long this will take.

The expected number of nodes that will become adopters in this time-step is the number of nodes that have not adopted the technology, $N(1-m)$, multiplied by this probability. The overall fraction of active nodes will therefore increase by

$$\Delta m = (1-m)P(Y \geq Y^*), \tag{4.10}$$

giving the updated value of $m(t+1)$ as a function of the current value $f(m(t))$:

$$m(t+1) = m(t) + (1-m(t))P(Y \geq Y^*) \equiv f(m(t)). \tag{4.11}$$

Y^* is also a function of m but, being an integer, can take only discrete values, so $f(m)$ is discontinuous when Y^* changes.

This gives a macroscopic, system-level, version of the microscopic (individual) dynamics given by (2.2). The functions in (4.11) and (4.10) are shown in Figure 3 for some example parameter values. In Figures 3(a) and (c) we have $Y^* > k = 6$ for $m < 0.1$, so $\Delta m = 0$ in this range, and starting at an initial seed level of $m_0 = 0.05$ will lead to stagnation. If $m_0 \geqslant 0.2$,

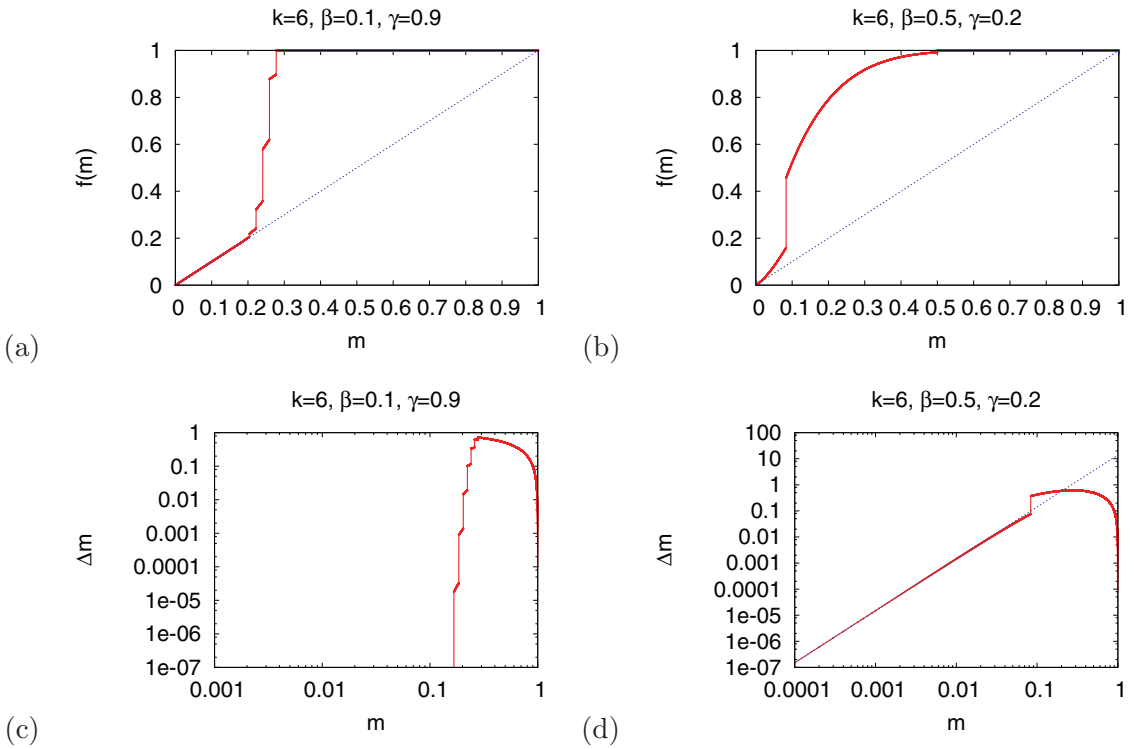

Figure 3. *Plots of* (4.11) *for* $k = 6$*:* (a) $\beta = 0.1, \gamma = 0.9$ *and* (b) $\beta = 0.5, \gamma = 0.2$. *Plots of* (4.10) *at the same values in* (c) *and* (d) *(on a log scale). In* (a) *and* (c) $Y^* > k$ *for small* m*, so there is no further uptake, and in* (b) *and* (d) $Y^* = 2$ *for small* m*, so uptake is disproportionately slow for small levels of seeding. The diagonal is drawn for comparison in* (a) *and* (b)*, while in* (d) *the fit to the initial slope is given.*

Δm is quite large, and success will come quickly. In contrast, in Figures 3(b) and (d), $Y^* = 2$ for small m, and uptake can happen only if the network size N is large enough to allow further nodes to be influenced.

For small values of the initial adoption $m \ll 1$ the following approximation can be made:

$$P(Y \geq Y^*) \approx \Delta m \approx \binom{k}{Y^*} m^{Y^*}, \tag{4.12}$$

with $Y^* \approx \left\lceil \bar{k} \left(\frac{\theta - \alpha p}{\beta} \right) \right\rceil$ for small enough m. If $Y^* > 1$, then the superlinear power of m results in very small returns for small initial seeding, and it takes a time on the order of $m_0^{1-Y^*}$ for a successful outcome for small m_0.

4.4. Structured networks. The approach above works for random networks, where independence of neighborhoods can be assumed, and for randomly distributed initial seeds. For networks with high clustering, where the clustering coefficient or *transitivity* [26, page 243], defined as

$$c = \left(\frac{3 \times \#(\text{triangles})}{\#(\text{length 2 paths})} \right), \tag{4.13}$$

is close to 1, this is not the case. This difference is demonstrated in the numerical simulations shown in Figure 4. For these results the Watts–Strogatz scheme was used to rewire a highly clustered one dimensional lattice, where nodes are initially laid out in a ring and linked to their six nearest neighbors. Due to the large number of triangles, this network has a high transitivity $c = 0.6$, indicating a 60% probability that any two neighbors of a node are also neighbors of each other. For comparison, a completely random ER network of this size and edge density would have $c = 0.01$.

The probability of rewiring is p_r, and for small values of p_r where there is still significant clustering, the results show successful uptake in around 50% of cases in the $Y^* = 3$ sector, with either successful or stagnated adoption for Y^* values below or above this, respectively. This behavior for $Y^* = 3$ would not be expected in random networks at these values, where the random probability of any particular neighborhood triggering an adoption $P(Y \geq Y^*) \approx 0.002$, resulting in only a single expected further uptake per realization. This would result in very slow uptake or stagnation on finite networks, which is indeed what happens for large p_r, where c is small and the network is again more random in structure (Figure 4(d)).

The enhanced success of uptake in these cases is due to the clustered structure favoring continuing propagation from any influential neighborhood. In clustered networks, any neighbor j of a newly activated node i is likely to also be a neighbor of the nodes that influenced i to adopt, and so j has an enhanced chance of becoming an adopter itself. If a suitable neighborhood is present under these circumstances, one uptake will then trigger another in an adjacent position due to this overlap of neighborhoods (see Figure 5). If clustering is sufficient that there is overlap between neighborhoods for a sizeable portion of the whole network, then it can take only a single critical neighborhood to induce a successful uptake for the system. The 50% chance of success seen in Figure 4(a) in the $Y^* = 3$ sector then represents the chance of randomly seeding a group of nodes in such a way as to trigger this process. The probability, given by (4.8), of at least one node in a random system having a critical neighborhood yields

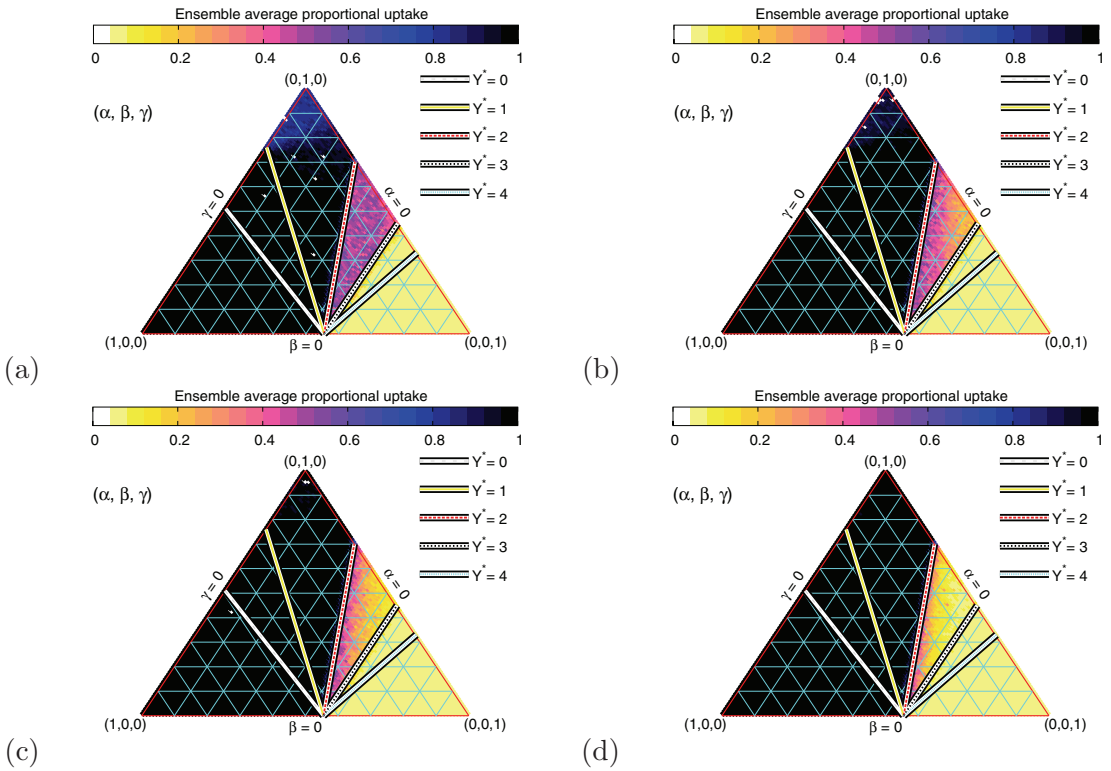

Figure 4. *Results on Watts–Strogatz networks with nodes initially connected to their six nearest neighbors on a one dimensional lattice and different rewiring probabilities p_r, resulting in different transitivity c:* (a) $p_r = 0$, $c = 0.6$; (b) $p_r = 0.01$, $c = 0.57$; (c) $p_r = 0.02$, $c = 0.53$; (d) $p_r = 0.05$, $c = 0.45$. *Model parameters are* $p = 0.5$ *and* $\theta = 0.25$, *with* $N = 500$. *Edges were swapped in pairs to preserve the node degree* $k = 6$.

$P(Z \geq 1) \approx 0.67$ for $k = 6$, $Y^* = 3$, and $N = 500$. Equation (4.8) is strictly valid only for independent neighborhoods and hence gives too high a value in this case, where neighborhoods overlap, but a quantitatively accurate expression would require a far more intensive calculation of the different combinations of the initial seed for the whole system. However, the current method is accurate enough to give qualitatively correct predictions.

The propagation via overlapping neighborhoods is a percolation phenomenon, similar to that seen in other studies [22], but one that percolates on *hyperedges* connecting *hypernodes* rather than via single links. Here, a hypernode is a complete subgraph of $Y^* + 1$ nodes, or a $(Y^* + 1)$-*clique*. Two hypernodes are connected if the two $(Y^* + 1)$-cliques have Y^* nodes in common. The implication is that if a hypernode becomes active, then every hypernode to which it is connected will also become active in the next time-step. This is shown in Figure 5 for propagation via 4-cliques where $Y^* = 3$, with a single uptake triggering others via their overlapping neighborhoods. Threshold models on clustered networks are discussed at length in Chapter 19 of Easley and Kleinberg's *Networks, Crowds, and Markets* [11] (including some useful references to the economics literature), motivated by coordination game models of microeconomic cooperation between individuals.

To demonstrate the transition between cluster-enabled propagation and stagnation, the

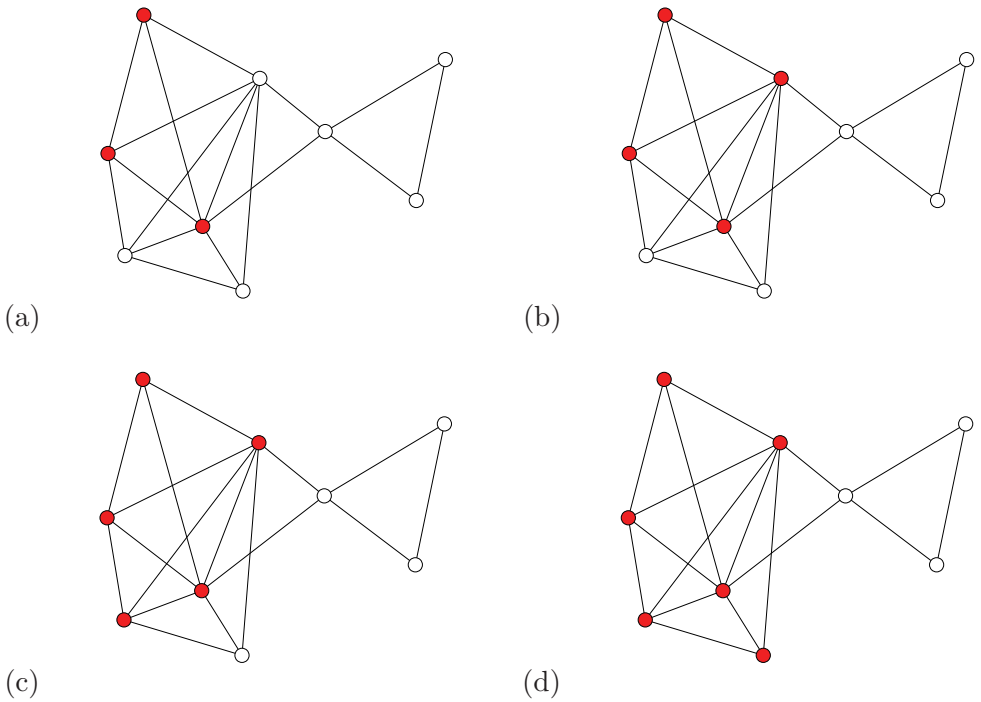

Figure 5. *An example of uptake propagation via clustering in a network where nodes require three active neighbors to become active themselves. The sequence of uptakes is shown in* (a)–(d)*, starting from a single node influenced by three of its neighbors, which then induces further uptake via* 3*-member overlap of* 4*-cliques.*

ensemble uptake within the $Y^* = 3$ sector of Figure 4 (after 36 time-steps) is shown in Figure 6, plotted as a function of both p_r and c. The regular (unrewired) network has a clustering coefficient $c = 0.6$, which decreases smoothly with increasing rewiring probability. If the node degree is held constant by rewiring edges in pairs (Figure 6(a)), then the average uptake after 36 time-steps fits well with the function $m(36) = \sigma \exp(\varepsilon c)$, with fitting parameters $\sigma = 2.9 \times 10^{-4}$ and $\varepsilon = 12.39$. This is not the case if edges are rewired one at a time (Figure 6(b)), where the node degree becomes distributed. In this case the uptake peaks at around 5% rewiring ($c \approx 0.5$), similar to other models showing a peak in the level of adoption at certain node degrees [1].

A further example is shown in Figure 7 for a community-based, random-clustered network [22], where the clustering can be varied by associating N individual nodes each via G groups of varying sizes M. The total number of communities W and number of connections L per individual in each community (here $L = 5$) determine the size and density of the communities and hence the amount of clustering. In Figure 7(d) the dependence of c on W is shown alongside the mean uptake after 36 time-steps, averaged over 1000 realizations for each W. Results similar to the previous case can be seen, with increased clustering resulting in an increased likelihood of successful uptake, despite the low number of influential neighborhoods. However, these expected values are valid only when averaging over different network realizations as well as initial adopters. For many networks it was found that uptake was almost never

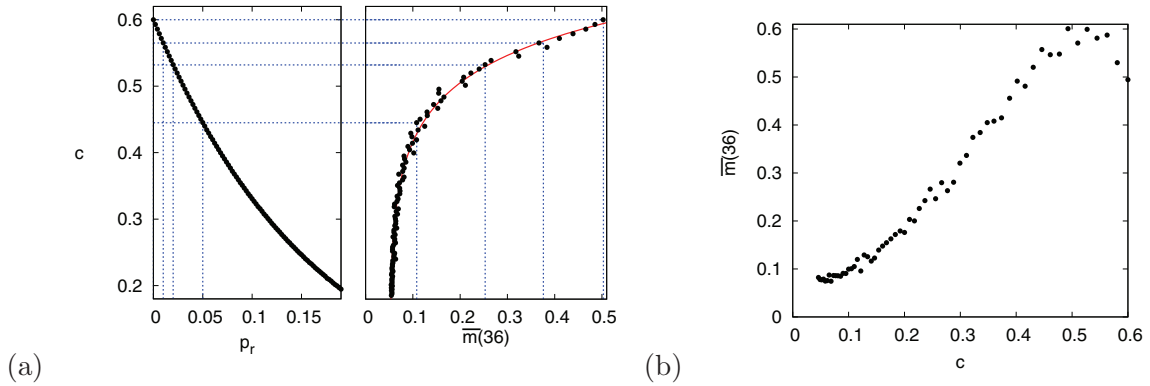

Figure 6. *Uptake on Watts–Strogatz rewired 6-neighbor rings, after 36 time-steps, against both rewiring probability p_r and clustering c.* (a) *Runs starting from 1000 random initial conditions with $m_0 = 0.05$, $\alpha = 0.1, \beta = 0.45, \gamma = 0.45, p = 0.5, \theta = 0.25$, randomizing the network on each realization. Edges are rewired in pairs to preserve the node degree $k = 6$. Dashed blue lines show the data in Figure 4, with $p_r = 0, 0.01, 0.02, 0.05$ and $c = 0.6, 0.57, 0.53, 0.45$, respectively. The fitted red curve is the function $\sigma \exp(\varepsilon c)$, with $\sigma = 2.9 \times 10^{-4}$, $\varepsilon = 12.39$.* (b) *For comparison, the same system is used but with edges rewired individually between $0 < p_r < 0.5$, showing the effect of allowing distribution of the node degree with p_r. A peak in the uptake appears at $c \approx 0.5$.*

achieved for most choices of initial adopters, which we believe to be related to the connectedness of cliques of size $Y^* + 1$. However, an interesting observation is the strong functional dependence of the expected success on the *transitivity*, which fits to about 1% accuracy to the function

$$m(36) = 1 - \sigma \exp(-\varepsilon c), \tag{4.14}$$

with fitting parameters $\sigma = 0.86$, $\varepsilon = 11.2$. This relationship was also found for different values of (α, β, γ) within the $Y^* = 3$ sector, with different coefficients in (4.14). This suggests that it is possible to obtain an analytical expression for these systems and should motivate further research.

The phenomenon of connectedness via more highly connected clusters than single edges is known as k-clique percolation, and results exist deriving this result for random ER networks [10, 24]. However, to understand the results in Figure 7 analytically would require results for the expected connected $(Y^* + 1)$-clique percolation component size distribution as a function of the clustering coefficient. Some progress has been made in this direction, with numerical results existing for cascades of various models, such as Watts' threshold model [27] on clustered random networks like the Newman model [18]. Additionally analytical results have also been derived for expected connected component sizes for single bond percolation on clustered networks [14]. However, obtaining the required results for k-clique percolation components remains an open and difficult problem.

These results imply that, in cases where several network neighbors are required to influence adoption, greater levels of system-wide adoption can be achieved in more highly clustered networks, in agreement with earlier results on similar systems [8]. Therefore, innovations in systems with more communication between overlapping groups of individuals will be more

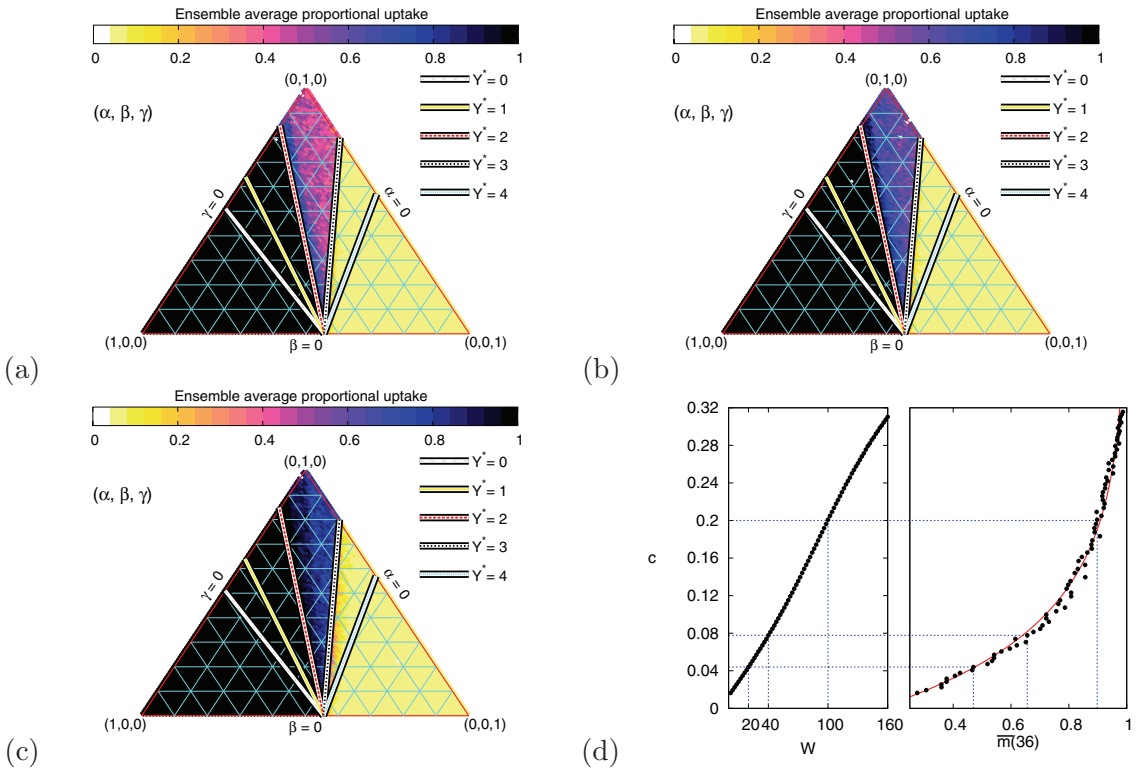

Figure 7. *Same as Figures 4 and 6 but for a community-based, Newman, random-clustered, network model. The network size $N = 500$, so for each number of groups W there are M members, on average, resulting in a measured transitivity c:* (a) $W = 20$, $M = 25$, $c = 0.044$, (b) $W = 40$, $M = 12.5$, $c = 0.078$, (c) $W = 100$, $M = 5$, $c = 0.2$. (d) *Clustering as a function of W versus uptake for $\alpha = 0.1, \beta = 0.8, \gamma = 0.1$ within the $Y^* = 3$ sector. The fitted red line is the empirical function $m(36) = 1 - \sigma \exp(-\varepsilon c)$, with $\sigma = 0.86$, $\varepsilon = 11.2$.*

likely to succeed than if such overlap were not present.

4.5. Scale-free networks. In the current model and analysis we have so far considered only networks with node degrees that are distributed close to the mean value. This is mainly due to the nature of the recommendation network being restricted to a close group of associates. However, it is possible to apply the multiparameter model used here to networks with broader degree distributions in order to compare the results and their generalizability. In such cases the fat-tails of the degree distribution strongly violate the requirement of our analysis (in section 4.1) that $\bar{k}$ be meaningful and represent most of the nodes in the network. The result of this is demonstrated in Figure 8 using Barabási–Albert networks, showing how the division between the regions of the parameter space becomes less clear than in the case of near-constant degree. In such cases the analysis presented here would not be applicable and would require a more sophisticated approach.

5. Conclusions. We have introduced a three parameter model for the diffusion of innovations by individuals connected by a network of peer-to-peer influences, and methods for the investigation and analysis of such models. This model has particular application to technologies with varying degrees of visibility, such as energy efficiency installations in households.

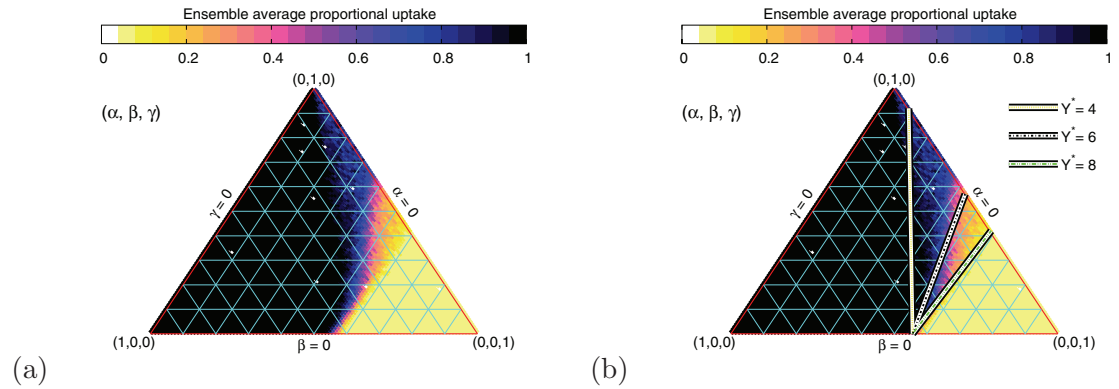

Figure 8. *Results on a* scale-free *Barabási–Albert network. The division between regions of the parameter space is less clearly defined and no longer linear, due to the broad degree distribution of the nodes.*

Numerical simulations have been carried out, computing the average uptake of an innovation over many realizations, to account for the sensitivity of network diffusion processes. This was carried out at a range of model parameter values on various network topologies and initial conditions. It has been found that the expected level of adoption depends strongly on the topology of the network and the Y^* sector that the (β, γ) parameters are in. The node degree and the network's transitivity, related to the correlation between the neighborhoods of connected individuals, were found to be of particular importance.

An analytical and probabilistic approach has been developed to account for the observed behavior. In the current work we have introduced the model, along with methods for investigating it and similar models, in its most tractable form. The analysis explains the results of the numerical calculations well in the case of randomly connected networks and provides useful insight in the case of networks with clustering. The study and the model here are limited to homogeneous nodes with the same parameters and equal weights. The analysis of the model also made use of the assumption of a near-constant node degree and so does not carry over simply to scale-free networks. In this work we argued that communication on innovation adoption is restricted to a select few contacts and therefore excludes wide degree distributions. An alternative would be to assume that individuals are influenced by a *number* rather than *fraction* of their network neighbors, which is independent of $\bar{k}$.

The dynamical adoption model can be made to account for the various archetypes discussed in the social science literature by assigning individuals to different groups. Individuals in different categories can be assigned different α_i, β_i, and γ_i values, depending on their personality, for example, with technology enthusiasts having high α values, social followers having high β, and cautious individuals having a high γ. In subsequent work we have extended the model to cases involving inhomogeneous nodes with distributions of parameters, weights, and degrees in order to study the sensitivity of the results to such factors [3].

The model provides a basis to simulate the behavior seen in the real world. For example, it can form the basis for computational investigations comparing different interventions by a government agency to try to improve the level of uptake of innovations relating to energy efficiency. These could be represented in the model by varying the initial seeding for different

roll-out strategies or varying the network structure for different word-of-mouth marketing campaigns. By identifying intervention strategies that have a high probability of achieving successful uptake of the technology, the model could allow government to make informed decisions on whether to go ahead with interventions and, if so, how. Such *interventions* are the subject of subsequent research by the authors [2] based on enhancing uptake, either by altering the parameters of the model or the network structure, in ways that have real-world interpretations.

In a similar way the effect of marketing could also be considered in a more general context. Such advertising would be an active attempt to promote, or enhance the perception of, the utility through one or more of the parameters or variables. This could be included as either a nonlinear function of $m(t)$ (currently a linear global (all–all) feedback from the system norm to the individuals) or another term that effectively increases u. Related models have used an external driver taking this role in addition to the feedback from other nodes [5], and this feature could easily be incorporated into our model. Additionally, the current model currently considers only a single innovation, but it would also be interesting to include features of competition between competing products in future developments.

Future studies could also modify the community-based network models to provide more flexibility and realistic features in a number of ways. Some positional information can be ascribed to the nodes and some or all of the groups, preferentially attaching individuals to communities that are geographically closer, in a similar way to Hamill and Gilbert's *social circles* model [19]. In cases where none (or only one) of the groups has geographic information, they again reduce to the Newman scheme. These groups could be classified into different categories; for example, some could have a fixed membership number to allow variation of the clustering between groups and represent different types of group interaction (e.g., social or workplace groups). For other types there could be no geographical element, introducing long-range connections into the network, as may be the case for workplaces. The model could also be given a stochastic element, either on the transfer of information along links (e.g., as in [5]), or by allowing a distribution of time-step values, as well as nonsynchronous updating, and introducing a probabilistic, rather than deterministic, uptake once the utility exceeds its threshold. A further feature of interest is that of nonstatic network topologies. Although the networks in the short time-scales investigated here have been assumed static, it is interesting to consider what effect dynamic networks would have on the adoption process. In our subsequent modeling work we have investigated cases where links are added to existing networks as the diffusion process is ongoing [2]. Depending on the nature of the dynamics of the network restructuring, there is potential for the added mixing to enhance uptake in these cases.

As well as the application of the diffusion of (energy) innovations that were used as a basis for this model, the methods discussed in this paper can also be applied to multiparameter models of different systems with similar features and can provide a framework for the investigation of many real-world systems.

Acknowledgments. The authors thank Mason Porter for some very useful discussions of this problem from the perspective of mean-field and probability approaches. The authors are also grateful for the considered and thoughtful comments and suggestions of the referees,

which have been very helpful in improving the manuscript and providing food for thought.

REFERENCES

[1] F. Alkemade and C. Castaldi, *Strategies for the diffusion of innovations on social networks*, Computational Economics, 25 (2005), pp. 3–23.

[2] C. S. E. Bale, N. J. McCullen, T. J. Foxon, A. M. Rucklidge, and W. F. Gale, *Harnessing social networks for promoting adoption of energy technologies in the domestic sector*, Complexity (special section arising from the Complexity Science in the Real World Network Conference), 2012, submitted.

[3] C. S. E. Bale, N. J. McCullen, T. J. Foxon, A. M. Rucklidge, and W. F. Gale, *Modelling diffusion of energy innovations on a social network and integration of real-world data*, Energy Policy, submitted.

[4] C. S. E. Bale, N. J. McCullen, T. J. Foxon, A. M. Rucklidge, and W. F. Gale, *Local authority interventions in the domestic sector and the role of social networks: A case study from the city of Leeds*, in UKERC Conference on Energy and People: Futures, Complexity and Challenges, 2011.

[5] D. S. Bassett, D. L. Alderson, and J. M. Carlson, *Collective decision dynamics in the presence of external drivers*, Phys. Rev. E, 86 (2012), 036105.

[6] S. Bikhchandani, D. Hirshleifer, and I. Welch, *A theory of fads, fashion, custom, and cultural change as informational cascades*, J. Political Economy, (1992), pp. 992–1026.

[7] C. Castellano, S. Fortunato, and V. Loreto, *Statistical physics of social dynamics*, Rev. Modern Phys., 81 (2009), pp. 591–646.

[8] H. Choi, S. H. Kim, and J. Lee, *Role of network structure and network effects in diffusion of innovations*, Industrial Marketing Management, 39 (2010), pp. 170–177.

[9] S. A. Delre, W. Jager, T. H. A. Bijmolt, and M. A. Janssen, *Will it spread or not? The effects of social influences and network topology on innovation diffusion*, J. Product Innovation Management, 27 (2010), pp. 267–282.

[10] I. Derényi, G. Palla, and T. Vicsek, *Clique percolation in random networks*, Phys. Rev. Lett., 94 (2005), 160202.

[11] D. Easley and J. Kleinberg, *Networks, Crowds, and Markets*, Cambridge University Press, Cambridge, UK, 2010.

[12] P. Erdős and A. Rényi, *On the evolution of random graphs*, Magyar Tud. Akad. Mat. Kutató Int. Közl., 5 (1960), pp. 17–61.

[13] J. P. Gleeson, *Cascades on correlated and modular random networks*, Phys. Rev. E, 77 (2008), 046117.

[14] J. P. Gleeson, *Bond percolation on a class of clustered random networks*, Phys. Rev. E, 80 (2009), 036107.

[15] J. P. Gleeson and D. J. Cahalane, *Seed size strongly affects cascades on random networks*, Phys. Rev. E, 75 (2007), 056103.

[16] J. P. Gleeson, S. Melnik, J. A. Ward, M. A. Porter, and P. J. Mucha, *Accuracy of mean-field theory for dynamics on real-world networks*, Phys. Rev. E, 85 (2012), 026106.

[17] M. Granovetter and R. Soong, *Threshold models of diffusion and collective behavior*, J. Math. Sociol., 9 (1983), pp. 165–179.

[18] A. Hackett, S. Melnik, and J. P. Gleeson, *Cascades on a class of clustered random networks*, Phys. Rev. E, 83 (2011), 056107.

[19] L. Hamill and N. Gilbert, *Social circles: A simple structure for agent-based social network models*, J. Artificial Societies Social Simul., 12 (2009); available online from http://jasss.soc.surrey.ac.uk/12/2/3.html.

[20] E. Lee, J. Lee, and J. Lee, *Reconsideration of the winner-take-all hypothesis: Complex networks and local bias*, Management Sci., 52 (2006), pp. 1838–1848.

[21] P. G. Lind and H. J. Herrmann, *New approaches to model and study social networks*, New J. Phys., 9 (2007), 228.

[22] M. E. J. Newman, *Properties of highly clustered networks*, Phys. Rev. E, 68 (2003), 026121.

[23] G. Palla, I. Derényi, I. Farkas, and T. Vicsek, *Uncovering the overlapping community structure of complex networks in nature and society*, Nature, 435 (2005), pp. 814–818.

[24] G. Palla, I. Derényi, and T. Vicsek, *The critical point of k-clique percolation in the Erdős–Rényi graph*, J. Stat. Phys., 128 (2007), pp. 219–227.
[25] T. W. Valente, *Social network thresholds in the diffusion of innovations*, Social Networks, 18 (1996), pp. 69–89.
[26] S. Wasserman and K. Faust, *Social Network Analysis: Methods and Applications*, Vol. 8, Cambridge University Press, Cambridge, UK, 1994.
[27] D. J. Watts, *A simple model of global cascades on random networks*, Proc. Natl. Acad. Sci. USA, 99 (2002), pp. 5766–5771.
[28] D. J. Watts and S. H. Strogatz, *Collective dynamics of 'small-world' networks*, Nature, 393 (1998), pp. 440–442.
[29] M. W. Weenig and C. J. Midden, *Communication network influences on information diffusion and persuasion*, J. Personality Social Psych., 61 (1991), p. 734.